

Baryonium Study in Heavy Baryon Chiral Perturbation Theory

Yue-De Chen^{a*} and Cong-Feng Qiao^{a,b†}

a) Department of Physics, Graduate University, the Chinese Academy of Sciences

YuQuan Road 19A, 100049, Beijing, China

b) Theoretical Physics Center for Science Facilities (TPCSF), CAS

YuQuan Road 19B, 100049, Beijing, China

To see whether heavy baryon and anti-baryon can form a bound state, the heavy baryonium, we study the two-pion exchange interaction potential between them within the heavy baryon chiral perturbation theory. The obtained potential is applied to calculate the heavy baryonium masses by solving the Schrödinger equation. We find it is true that the heavy baryonium may exist in a reasonable choice of input parameters. The uncertainties remaining in the potential and their influences on the heavy baryonium mass spectrum are discussed.

1 Introduction

Quark model has achieved great success in describing the experimentally observed hadronic structures to a large extent. And the quark potential in between quark and anti-quark deduced from Chromodynamics (QCD) can explain the meson spectrum quite well. Many of predicted states by potential model were discovered in experiment and the theoretical predictions are in good agreement with experimental data, especially in

*Email: chenyuède-b07@mails.gucas.ac.cn

†Email: qiaocf@gucas.ac.cn

charmonium and bottomonium sectors [1, 2, 3], where the masses of charm and bottom quarks are heavy enough to be treated non-relativistically. However, things became confused after the discovery of $X(3872)$ in 2003 at Belle [4], which was later confirmed by BaBar [5]. In recent years, a series of unusual states in charmonium sector, such as $Y(4260)$, $Y(4360)$, $Y(4660)$, and $Z^\pm(4430)$, were observed in experiment [6]. Due to their extraordinary decay nature, it is hard to embed them into the conventional charmonium spectrum, which leads people to treat them as exotic rather than quark-quark bound states. The typical scenarios in explaining these newly found states include treating $Y(4260)$ as a hybrid charmonium [7], a $\chi_c\rho^0$ molecular state [8], a conventional $\Psi(4S)$ [9], an $\omega\chi_{c1}$ molecular state [10], a $\Lambda_c\bar{\Lambda}_c$ baryonium state [11], a D_1D or D_0D^* hadronic molecule [12], and a P -wave tetraquark $[cs][\bar{c}\bar{s}]$ state [13]; $Y(4360)$ is interpreted as the candidate of the charmonium hybrid or an excited D-wave charmonium state, the 3^3D_1 [14] and an excited state of baryonium [16]; $Y(4660)$ is suggested to be the excited S-wave charmonium states, the 5^3S_1 [14] and 6^3S_1 [15], a baryonium state [16, 17], a $f_0(980)\Psi'$ bound state [18, 19], a 5^3S_1 - 4^3D_1 mixing state [20], and also a tetraquark state [21, 22]. There have been recently many research works on "exotic" heavy quarkonium study in experiment and theory. To know more of recent progress in this respect and to have a more complete list of references one can see e.g. recent reviews [23, 24] and references therein.

In the baryonium picture, the tri-quark clusters are baryon-like, but not necessarily colorless. In the pioneer works of heavy baryonium for the interpretation of newly observed "exotic" structures [11, 16], there were only phenomenological and kinematic analysis, but without dynamics. In this work we attempt to study the heavy baryonium interaction potential arising from two-pion exchanges in the framework of Heavy Baryon Chiral Perturbation Theory (HBCPT) [25]. The paper is organized as follows. In Section 2, we present the formalism for the heavy baryon-baryon interaction study; in Section 3 we perform the numerical study for the mass spectrum of the possible baryonium with the obtained potential in preceding section; the Section 4 is devoted to the summary and conclusions. For the sake of reader's convenience some of the used formulae are given in the Appendix.

2 Formalism

To obtain the heavy baryonium mass spectrum, we first start from extracting the baryon-baryon interaction potential in the same procedure as for quark-quark interaction [1].

2.1 Heavy Baryonium

In the heavy baryonium picture [16], Λ_c and Σ_c^0 are taken as basis vectors in two-dimensional space. The baryonia are loosely bound states of heavy baryon and anti-baryon, namely

$$\begin{aligned} B_1^+ &\equiv |\Lambda_c^+ \bar{\Sigma}_c^0 \rangle \\ \text{Triplet : } B_1^0 &\equiv \frac{1}{\sqrt{2}}(|\Lambda_c^+ \bar{\Lambda}_c^+ \rangle - |\Sigma_c^0 \bar{\Sigma}_c^0 \rangle) \\ B_1^- &\equiv |\bar{\Lambda}_c^+ \Sigma_c^0 \rangle \end{aligned} \quad (1)$$

and

$$\text{Singlet : } B_0^0 \equiv \frac{1}{\sqrt{2}}(|\Lambda_c^+ \bar{\Lambda}_c^+ \rangle + |\Sigma_c^0 \bar{\Sigma}_c^0 \rangle) . \quad (2)$$

Here, approximately the transformation in this two-dimensional "C-spin" space is invariant, which is in analog to the invariance of isospin transformation in proton and neutron system.

2.2 Effective Chiral Lagrangian

Heavy baryon contains both light and heavy quarks, of which the light component exhibits the chiral property and the heavy component exhibits heavy symmetry. Therefore, it is plausible to tackle the problem of heavy baryon interaction through the heavy chiral perturbation theory. Following we briefly review the gists of the HBCPT for later use.

In usual chiral perturbation theory, the nonlinear chiral symmetry is realized by making use of the unitary matrix

$$\Sigma = e^{\frac{2iM}{f_\pi}} , \quad (3)$$

where M is a 3×3 matrix composed of eight Goldstone-boson fields, i.e.,

$$M = \begin{pmatrix} \frac{1}{\sqrt{2}}\pi^0 + \frac{1}{\sqrt{6}}\eta & \pi^+ & K^+ \\ \pi^- & -\frac{1}{\sqrt{2}}\pi^0 + \frac{1}{\sqrt{6}}\eta & K^0 \\ K^- & \bar{K}^0 & -\frac{2}{\sqrt{6}}\eta \end{pmatrix}. \quad (4)$$

Here, f_π is the *pion* decay constant.

After the chiral symmetry spontaneously broken, the Goldstone boson interaction with hadron is introduced through a new matrix [26, 27]

$$\xi = \Sigma^{\frac{1}{2}} = e^{\frac{iM}{f_\pi}}. \quad (5)$$

From ξ one can construct a vector field V_μ and an axial vector field A_μ with simple chiral transformation properties, i.e.,

$$V_\mu = \frac{1}{2}(\xi^\dagger \partial_\mu \xi + \xi \partial_\mu \xi^\dagger), \quad (6)$$

$$A_\mu = \frac{i}{2}(\xi^\dagger \partial_\mu \xi - \xi \partial_\mu \xi^\dagger). \quad (7)$$

For our aim, we work only on the leading order vector and axial vector fields in the expansion of ξ in terms of f_π , they are

$$V_\mu = \frac{1}{f_\pi^2} M \partial_\mu M, \quad (8)$$

$$A_\mu = -\frac{1}{f_\pi} \partial_\mu M. \quad (9)$$

For heavy baryon, each of the two light quarks is in a triplet of flavor SU(3), and hence the baryons can be grouped in two different SU(3) multiplets, the sextet and antitriplet. The symmetric sextet and antisymmetric triplet can be constructed out in 3×3 matrices [27], they are

$$B_6 = \begin{pmatrix} \Sigma_c^{++} & \frac{1}{\sqrt{2}}\Sigma_c^+ & \frac{1}{\sqrt{2}}\Xi_c'^+ \\ \frac{1}{\sqrt{2}}\Sigma_c^+ & \Sigma_c^0 & \frac{1}{\sqrt{2}}\Xi_c'^0 \\ \frac{1}{\sqrt{2}}\Xi_c'^+ & \frac{1}{\sqrt{2}}\Xi_c'^0 & \Omega_c^0 \end{pmatrix}, \quad (10)$$

and

$$B_{\bar{3}} = \begin{pmatrix} 0 & \Lambda_c & \Xi_c^+ \\ -\Lambda_c & 0 & \Xi_c^- \\ -\Xi_c^+ & -\Xi_c^- & 0 \end{pmatrix}, \quad (11)$$

respectively.

Introducing six coupling constant g_i , $i = 1, 6$, the general chiral-invariant Lagrangian then reads [25]

$$\begin{aligned}
\mathcal{L}_{\mathcal{G}} = & \frac{1}{2}tr[\bar{B}_3(i\not{D} - M_3)B_3] + tr[\bar{B}_6(i\not{D} - M_6)B_6] \\
& + tr[\bar{B}_6^{*\mu}[-g_{\mu\nu}(i\not{D} - M_6^*) + i(\gamma_\mu\not{D}_\nu + \gamma_\nu\not{D}_\mu) - \gamma_\mu(i\not{D} + M_6^*)\gamma_\nu]B_6^{*\nu}] \\
& + g_1tr(\bar{B}_6\gamma_\mu\gamma_5A^\mu B_6) + g_2tr(\bar{B}_6\gamma_\mu\gamma_5A^\mu B_3) + h.c. \\
& + g_3tr(\bar{B}_{6\mu}^*A^\mu B_6) + h.c. + g_4tr(\bar{B}_{6\mu}^*A^\mu B_3) + h.c. \\
& + g_5tr(\bar{B}_6^{\nu*}\gamma_\mu\gamma_5A^\mu B_{6\nu}^*) + g_6tr(\bar{B}_3\gamma_\mu\gamma_5A^\mu B_3) .
\end{aligned} \tag{12}$$

Here, $B_{6\nu}^*$ is a Rarita-Schwinger vector-spinor field for spin- $\frac{3}{2}$ particle; M_3 , M_6 , M_6^* represent for heavy baryon mass matrices of corresponding fields; With the help of vector current V_μ defined in Eq. (8), we may construct the covariant derivative D_μ , which acts on baryon field, as

$$D_\mu B_6 = \partial_\mu B_6 + V_\mu B_6 + B_6 V_\mu^T , \tag{13}$$

$$D_\mu B_3 = \partial_\mu B_3 + V_\mu B_3 + B_3 V_\mu^T , \tag{14}$$

where V_μ^T stands for the transpose of V_μ . Thus, the couplings of vector current to heavy baryons relevant to our task take the following form

$$\begin{aligned}
\mathcal{L}_{\mathcal{E}_1} &= \frac{1}{2}tr(\bar{B}_3 i\gamma^\mu V_\mu B_3) \\
&= \frac{1}{2f_\pi^2}\bar{\Lambda}_c i\gamma^\mu (\pi^0\partial_\mu\pi^0 + \pi^-\partial_\mu\pi^+ + \pi^+\partial_\mu\pi^-)\Lambda_c ,
\end{aligned} \tag{15}$$

and

$$\begin{aligned}
\mathcal{L}_{\mathcal{E}_2} &= \frac{1}{2}tr(\bar{B}_3 B_3 i\gamma^\mu V_\mu^T) \\
&= \frac{1}{2f_\pi^2}\bar{\Lambda}_c \Lambda_c i\gamma^\mu (\pi^0\partial_\mu\pi^0 + \pi^-\partial_\mu\pi^+ + \pi^+\partial_\mu\pi^-) .
\end{aligned} \tag{16}$$

According to the heavy quark symmetry, there are four constraint relations among those six coupling constants of the Lagrangian of Eq. (12), i.e.,

$$g_6 = 0 , \quad g_3 = \frac{\sqrt{3}}{2}g_1 , \quad g_5 = -\frac{3}{2}g_1 , \quad g_4 = -\sqrt{3}g_2 , \tag{17}$$

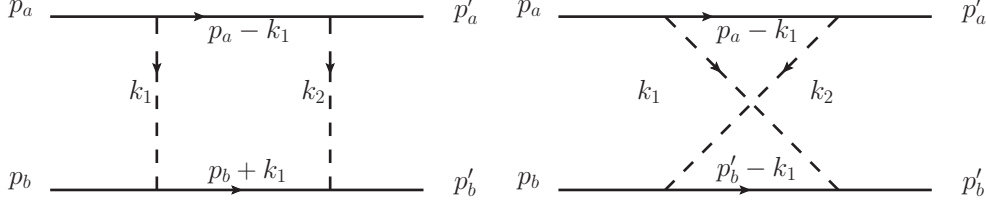


Figure 1: Schematic Diagrams which contribute to the baryonium potential.

which means the number of independent couplings are then reduced to two. In this work, we employ g_1 and g_2 for the numerical evaluation as did in Ref. [25].

Here, to get the dominant interaction potential we restrict our effort only on the *pion* exchange processes as usual. Notice that the couplings of *pion* to spin- $\frac{3}{2}$ and $-\frac{1}{2}$ baryons, and *pion* to two spin- $\frac{1}{2}$ baryons take a similar form, in the following we merely present the spin- $\frac{3}{2}$ and $-\frac{1}{2}$ baryon-*pion* coupling for illustration, i.e.,

$$\mathcal{L}_1 = \frac{g_3}{\sqrt{2}f_\pi} \bar{\Sigma}_c^{0*\mu} \partial_\mu \pi^0 \Sigma_c^0 + h.c. , \quad (18)$$

$$\mathcal{L}_2 = -\frac{g_3}{\sqrt{2}f_\pi} \bar{\Sigma}_c^{+*\mu} \partial_\mu \pi^+ \Sigma_c^0 + h.c. , \quad (19)$$

$$\mathcal{L}_3 = \frac{g_4}{f_\pi} \bar{\Sigma}_c^{++*\mu} \partial_\mu \pi^+ \Lambda_c^+ + h.c. , \quad (20)$$

$$\mathcal{L}_4 = -\frac{g_4}{f_\pi} \bar{\Sigma}_c^{0*\mu} \partial_\mu \pi^- \Lambda_c^+ + h.c. , \quad (21)$$

$$\mathcal{L}_5 = -\frac{g_4}{f_\pi} \bar{\Sigma}_c^{+*\mu} \partial_\mu \pi^0 \Lambda_c^+ + h.c. . \quad (22)$$

To get the *pion* and two spin- $\frac{1}{2}$ baryon couplings one only needs to replace the $\Sigma_c^{*\mu}$ by Σ_c , g_3 by g_1 , g_4 by g_2 , and insert $\gamma^\mu \gamma_5$ in between the two baryon fields in Eqs.(18)-(22).

2.3 Baryonium Potential from Two-pion Exchange

To obtain heavy baryon-baryon interaction potential in configuration space, we start from writing down the two-body scattering amplitude in the center-of-mass frame(CMS), i.e. taking $\mathbf{p}_a = -\mathbf{p}_b$ and $\mathbf{p}'_a = -\mathbf{p}'_b$. In CMS the total and relative four momenta are

defined as

$$P = (p_a + p_b) = (p'_a + p'_b) = (E, 0) , \quad (23)$$

$$p = \frac{1}{2}(p_a - p_b) = (0, \mathbf{p}) , \quad (24)$$

$$p' = \frac{1}{2}(p'_a - p'_b) = (0, \mathbf{p}') . \quad (25)$$

To perform the calculation, it is convenient to introduce some new variables as functions of \mathbf{p} and \mathbf{p}' , i.e.,

$$\mathcal{W}(\mathbf{p}) = E_a(\mathbf{p}) + E_b(\mathbf{p}) , \quad (26)$$

$$\mathcal{W}(\mathbf{p}') = E_a(\mathbf{p}') + E_b(\mathbf{p}') , \quad (27)$$

$$F_E(\mathbf{p}, p_0) = \frac{1}{2}E + p_0 - E(\mathbf{p}) + i\delta , \quad (28)$$

where δ is an infinitesimal quantity introduced in the so-called $i\delta$ prescription. Following the same procedure as in Refs. [28, 29], it is straightforward to write down the baryon-baryon scattering kernels, shown as box and crossed diagrams in Figure 1,

$$\begin{aligned} K_{box} = & - \frac{1}{(2\pi)^2} (E - \mathcal{W}(\mathbf{p}')) (E - \mathcal{W}(\mathbf{p})) \int dp'_0 dp_0 dk_{20} dk_{10} d^3\mathbf{k}_2 d^3\mathbf{k}_1 \\ & \times \frac{i}{(2\pi)^4} \delta^4(p - p' - k_1 - k_2) \frac{1}{k_2^2 - m^2 + i\delta} \frac{1}{F_E(\mathbf{p}', p'_0) F_E(-\mathbf{p}', -p'_0)} \\ & \times \frac{\Gamma_j \Gamma_i \Gamma_i \Gamma_j}{F_E(\mathbf{p} - \mathbf{k}, p_0 - k_{10}) F_E(-\mathbf{p} + \mathbf{k}, -p_0 + k_{10})} \frac{1}{F_E(\mathbf{p}, p_0) F_E(\mathbf{p}, -p_0)} \\ & \times \frac{1}{k_1^2 - m^2 + i\delta} , \end{aligned} \quad (29)$$

$$\begin{aligned} K_{cross} = & - \frac{1}{(2\pi)^2} (E - \mathcal{W}(\mathbf{p}')) (E - \mathcal{W}(\mathbf{p})) \int dp'_0 dp_0 dk_{20} dk_{10} d^3\mathbf{k}_2 d^3\mathbf{k}_1 \\ & \times \frac{i}{(2\pi)^4} \delta^4(p - p' - k_1 - k_2) \frac{1}{k_2^2 - m^2 + i\delta} \frac{1}{F_E(\mathbf{p}', p'_0) F_E(-\mathbf{p}', -p'_0)} \\ & \times \frac{\Gamma_j \Gamma_i \Gamma_j \Gamma_i}{F_E(\mathbf{p} - \mathbf{k}, p_0 - k_{10}) F_E(-\mathbf{p}' - \mathbf{k}, -p'_0 - k_{10})} \frac{1}{F_E(\mathbf{p}, p_0) F_E(-\mathbf{p}, -p_0)} \\ & \times \frac{1}{k_1^2 - m^2 + i\delta} . \end{aligned} \quad (30)$$

Here, m corresponds to the *pion* mass and $\Gamma_{i,j}$ are heavy baryon-*pion* interaction vertices that can be read out from the Lagrangian in Eqs.(18)-(22). In case of spin- $\frac{3}{2}$ intermediate,

$$\begin{aligned}\Gamma_j \Gamma_i \Gamma_i \Gamma_j &= \left(\frac{g_4}{f_\pi} \right)^4 \bar{u}(-p) k_2^\mu u_\mu(p-k_1) \bar{u}_\nu(p-k_1) k_1^\nu u(p) \\ &\times \bar{v}(p) (-k_1^\alpha) v_\alpha(-p+k_1) \bar{v}_\beta(-p+k_1) k_2^\beta v(-p),\end{aligned}\quad (31)$$

and in case of spin- $\frac{1}{2}$ intermediate

$$\begin{aligned}\Gamma_j \Gamma_i \Gamma_i \Gamma_j &= \left(\frac{g_2}{f_\pi} \right)^4 \bar{u}(-p) \gamma_\mu \gamma_5 k_2^\mu u(p-k_1) \bar{u}(p-k_1) \gamma_\nu \gamma_5 k_1^\nu u(p) \\ &\times \bar{v}(p) \gamma_\alpha \gamma_5 (-k_1^\alpha) v(-p+k_1) \bar{v}(-p+k_1) \gamma_\beta \gamma_5 k_2^\beta v(-p).\end{aligned}\quad (32)$$

Integrating over p'_0 , p_0 , k_{10} , and k_{20} in Eq.(29) one obtains the interaction kernel of box diagram at order $\mathcal{O}(\frac{1}{M_H})$,

$$\begin{aligned}K_{box} &= - \frac{1}{(2\pi)^3} \int \frac{d^3 \mathbf{k}_1 d^3 \mathbf{k}_2}{4E_{\mathbf{k}_1} E_{\mathbf{k}_2}} \frac{\Gamma_j \Gamma_i}{E_{\mathbf{p}-\mathbf{k}_1} + E_{\mathbf{p}} - W + E_{\mathbf{k}_1}} \\ &\times \frac{\Gamma_i \Gamma_j}{E'_{\mathbf{p}} + E_{\mathbf{p}-\mathbf{k}_1} - W + E_{\mathbf{k}_2}} \frac{1}{E_{\mathbf{p}} + E_{\mathbf{p}'} - W + E_{\mathbf{k}_1} + E_{\mathbf{k}_2}},\end{aligned}\quad (33)$$

where M_H represents one of the heavy baryon mass, $M_{\Lambda_c^+}$, $M_{\Sigma_c^0}$ or $M_{\Sigma_c^{*}}$; $E_{\mathbf{p}-\mathbf{k}_1} = \sqrt{(\mathbf{p}-\mathbf{k}_1)^2 + M_{\Sigma_c^*}^2}$ is the intermediate state energy; $E_{\mathbf{k}_1} = \sqrt{\mathbf{k}_1^2 + m^2}$ and $E_{\mathbf{k}_2} = \sqrt{\mathbf{k}_2^2 + m^2}$ are two *pions*' energies; and $W = 2E(\mathbf{p})$. With the same procedure, we can get the interaction kernel of crossed diagram, i.e.

$$\begin{aligned}K_{cross} &= - \frac{1}{(2\pi)^3} \int \frac{d^3 \mathbf{k}_1 d^3 \mathbf{k}_2}{4E_{\mathbf{k}_1} E_{\mathbf{k}_2}} \frac{\Gamma_j \Gamma_i}{E_{\mathbf{p}-\mathbf{k}_1} + E_{\mathbf{p}} - W + E_{\mathbf{k}_1}} \\ &\times \frac{\Gamma_j \Gamma_i}{E'_{\mathbf{p}} + E_{\mathbf{p}'+\mathbf{k}_1} - W + E_{\mathbf{k}_1}} \frac{1}{E_{\mathbf{p}} + E_{\mathbf{p}'} - W + E_{\mathbf{k}_1} + E_{\mathbf{k}_2}}.\end{aligned}\quad (34)$$

Next, since what we are interested in is the heavy baryons, we can further implement the non-relativistic reduction on spinors with the help of vertices given in Eqs.(18)-(22). In the end, the non-relativistic reduction for $\Lambda_c^+ \Sigma_c^{+*} \pi^0$ and $\Lambda_c^+ \Sigma_c^+ \pi^0$ couplings gives

$$i \left(\frac{g_4}{f_\pi} \right) \bar{u}(p_2) u_\mu(p_1) (p_2 - p_1)^\mu = -i \left(\frac{g_4}{f_\pi} \right) \mathbf{S}^\dagger \cdot \mathbf{q}, \quad (35)$$

and

$$i \left(\frac{g_2}{f_\pi} \right) \bar{u}(p_2) \gamma_\mu \gamma_5 u(p_1) (p_2 - p_1)^\mu = i \left(\frac{g_2}{f_\pi} \right) \boldsymbol{\sigma}_1 \cdot \mathbf{q}, \quad (36)$$

respectively. Here, $\mathbf{q} = \mathbf{p}_2 - \mathbf{p}_1$ and \mathbf{S}^\dagger is the spin- $\frac{1}{2}$ to spin- $\frac{3}{2}$ transition operator.

In the process of deriving $\Lambda_c^+ - \bar{\Lambda}_c^+$ potential, the Σ_c^+ and Σ_c^{+*} are taken into account as intermediate states. Using Eqs. (35)-(36) and the explicit forms of spinors given in the appendix, we can readily obtain the reduction forms for the Σ_c^+ intermediate

$$\begin{aligned} & \bar{u}(-p)\gamma_\mu\gamma_5k_2^\mu u(p-k_1)\bar{u}(p-k_1)\gamma_\nu\gamma_5k_1^\nu u(p) \times \\ & \bar{v}(p)\gamma_\alpha\gamma_5(-k_1^\alpha)v(-p+k_1)\bar{v}(-p+k_1)\gamma_\beta\gamma_5k_2^\beta v(-p) \\ = & (\mathbf{k}_1 \cdot \mathbf{k}_2)^2 + (\boldsymbol{\sigma}_1 \cdot \mathbf{k}_1 \times \mathbf{k}_2)(\boldsymbol{\sigma}_2 \cdot \mathbf{k}_1 \times \mathbf{k}_2), \end{aligned} \quad (37)$$

the Σ_c^{+*} intermediate in the box diagram

$$\begin{aligned} & \bar{u}(-p)k_2^\mu u_\mu(p-k_1)\bar{u}_\nu(p-k_1)k_1^\nu u(p) \times \\ & \bar{v}(p)(-k_1^\alpha)v_\alpha(-p+k_1)\bar{v}_\beta(-p+k_1)k_2^\beta v(-p) \\ = & \frac{4}{9}(\mathbf{k}_1 \cdot \mathbf{k}_2)^2 - \frac{1}{9}(\boldsymbol{\sigma}_1 \cdot \mathbf{k}_1 \times \mathbf{k}_2)(\boldsymbol{\sigma}_2 \cdot \mathbf{k}_1 \times \mathbf{k}_2), \end{aligned} \quad (38)$$

and the crossed diagram

$$\begin{aligned} & \bar{u}(-p)k_2^\mu u_\mu(p-k_1)\bar{u}_\nu(p-k_1)k_1^\nu u(p) \times \\ & \bar{v}(p)(-k_1^\alpha)v_\alpha(-p+k_1)\bar{v}_\beta(-p+k_1)k_2^\beta v(-p) \\ = & \frac{4}{9}(\mathbf{k}_1 \cdot \mathbf{k}_2)^2 + \frac{1}{9}(\boldsymbol{\sigma}_1 \cdot \mathbf{k}_1 \times \mathbf{k}_2)(\boldsymbol{\sigma}_2 \cdot \mathbf{k}_1 \times \mathbf{k}_2), \end{aligned} \quad (39)$$

respectively. Thus, the spinor reduction finally leads to an operator $\mathcal{O}_1(\mathbf{k}_1, \mathbf{k}_2)$, of which the variables \mathbf{k}_1 and \mathbf{k}_2 can be replaced by gradient operators $\boldsymbol{\nabla}_1$ and $\boldsymbol{\nabla}_2$ in configuration space and acting on \mathbf{r}_1 and \mathbf{r}_2 , respectively. This operator is expressed as

$$\begin{aligned} \mathcal{O}_1(\mathbf{k}_1, \mathbf{k}_2) &= c_1 O_1(\mathbf{k}_1, \mathbf{k}_2) + c_2 O_2(\mathbf{k}_1, \mathbf{k}_2) \\ &= c_1(\mathbf{k}_1 \cdot \mathbf{k}_2)^2 + c_2(\boldsymbol{\sigma}_1 \cdot \mathbf{k}_1 \times \mathbf{k}_2)(\boldsymbol{\sigma}_2 \cdot \mathbf{k}_1 \times \mathbf{k}_2). \end{aligned} \quad (40)$$

Here, the decomposition coefficients c_1 and c_2 are given in Table 1. The first part of Eq. (40) may generate the central potential and the second part may generate the spin-spin coupling and the tensor potentials, which are explicitly shown in the Appendix.

Table 1: The values of coefficients c_1 and c_2 in the decomposition of operator $O(\mathbf{k}_1, \mathbf{k}_2)$ in Eq. (40). The left one is for the spin- $\frac{1}{2}$ intermediate state case and the right one is for the spin- $\frac{3}{2}$ case.

spin-1/2	c_1	c_2	spin-3/2	c_1	c_2
box	1	1	box	4/9	-1/9
cross	1	1	cross	4/9	1/9

To get the leading order central potential, e.g. for $\Lambda_c\bar{\Lambda}_c$ system, we first expand the energy in powers of $\frac{1}{M_H}$, but keep only the leading term, like

$$\frac{1}{E_{\mathbf{p}-\mathbf{k}_1} + E_{\mathbf{p}} - W + E_{\mathbf{k}_1}} \approx \frac{1}{M_{\Sigma_c^*} + M_{\Lambda_c} - 2M_{\Lambda_c} + E_{\mathbf{k}_1}} = \frac{1}{E_{\mathbf{k}_1} + \Delta_1}, \quad (41)$$

where $\Delta_1 = M_{\Sigma_c^*} - M_{\Lambda_c}$ represents the mass splitting. By virtue of the factorization in integrals given in the Appendix, we can then make a double Fourier transformation, i.e.,

$$V_C^B(r_1, r_2) = - \left(\frac{g_4^4}{f_\pi^4} \right) \int \int \frac{d^3\mathbf{k}_1 d^3\mathbf{k}_2}{(2\pi)^6} \frac{\mathcal{O}_1(\mathbf{k}_1, \mathbf{k}_2) e^{i\mathbf{k}_1 \mathbf{r}_1} e^{i\mathbf{k}_2 \mathbf{r}_2} f(\mathbf{k}_1^2) f(\mathbf{k}_2^2)}{2E_{\mathbf{k}_1} E_{\mathbf{k}_2} (E_{\mathbf{k}_1} + \Delta_1)(E_{\mathbf{k}_2} + \Delta_1)(E_{\mathbf{k}_1} + E_{\mathbf{k}_2})}, \quad (42)$$

where the superscript B denotes the box diagram and the subscript C means central potential. Similarly, one can get the central potential from the crossed diagram contribution

$$V_C^C(r_1, r_2) = - \left(\frac{g_4^4}{f_\pi^4} \right) \int \int \frac{d^3\mathbf{k}_1 d^3\mathbf{k}_2}{(2\pi)^6} \mathcal{O}_1(\mathbf{k}_1, \mathbf{k}_2) e^{i\mathbf{k}_1 \mathbf{r}_1} e^{i\mathbf{k}_2 \mathbf{r}_2} f(\mathbf{k}_1^2) f(\mathbf{k}_2^2) D, \quad (43)$$

where the superscript C denote crossed diagram and the subscript C means central potential, and

$$D = \frac{1}{4E_{\mathbf{k}_1} E_{\mathbf{k}_2}} \left[\left(\frac{1}{(E_{\mathbf{k}_1} + \Delta_1)^2} + \frac{1}{(E_{\mathbf{k}_2} + \Delta_1)^2} \right) \frac{1}{E_{\mathbf{k}_1} + E_{\mathbf{k}_2}} + \left(\frac{1}{(E_{\mathbf{k}_1} + \Delta_1)^2} + \frac{1}{(E_{\mathbf{k}_2} + \Delta_1)^2} + \frac{2}{(E_{\mathbf{k}_1} + \Delta_1)(E_{\mathbf{k}_2} + \Delta_1)} \right) \frac{1}{E_{\mathbf{k}_1} + E_{\mathbf{k}_2} + 2\Delta_1} \right] \quad (44)$$

In order to regulate the potentials we have introduced form factors at each baryon-pion vertex. The resulting $f(\mathbf{k}^2)$ form factors appearing in Eqs. (42) and (43) will be given in Section 3.

Taking a similar approach as given in above one can readily get the central potential in other interaction channels and also the tensor potential. Notice that although there exists the one-pion exchange contribution in $\Sigma_c\text{-}\Sigma_c$ system, due to the $\gamma_\mu\gamma_5$ nature in

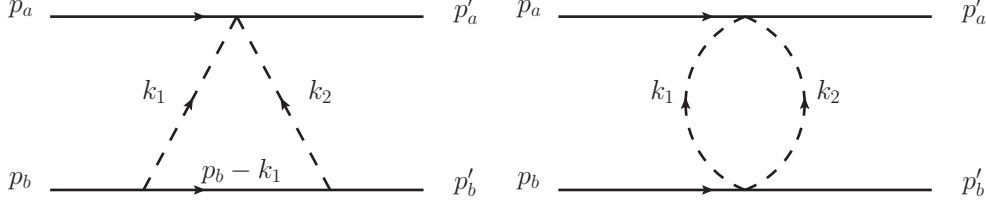


Figure 2: The triangle and two-pion loop diagrams.

interaction vertex, it only contributes to $\sigma_1 \cdot \sigma_2$ term, which is out of our concern in this work. Here we just focus on the central potential.

Besides box and crossed diagrams, there are also contributions from triangle and two-pion loop diagrams as shown in Fig. 2. As in the box and crossed diagrams, after integrating over energy component, we get the pion-pair contribution, as shown in the left diagram of Figure 2, as [33]

$$V_{triangle}(r_1, r_2) = \frac{g_4^2}{2f_\pi^4} \int \int \frac{d^3\mathbf{k}_1 d^3\mathbf{k}_2}{(2\pi)^6} \frac{\mathcal{O}_2(\mathbf{k}_1, \mathbf{k}_2)(E_{\mathbf{k}_1} + E_{\mathbf{k}_2})e^{i\mathbf{k}_1\mathbf{r}_1}e^{i\mathbf{k}_2\mathbf{r}_2}f(\mathbf{k}_1^2)f(\mathbf{k}_2^2)}{E_{\mathbf{k}_1}E_{\mathbf{k}_2}(E_{\mathbf{k}_1} + \Delta_1)(E_{\mathbf{k}_2} + \Delta_1)}, \quad (45)$$

where the $\mathcal{O}_2(\mathbf{k}_1, \mathbf{k}_2) = (\mathbf{k}_1 \cdot \mathbf{k}_2)$ from spinor reduction can be replaced in configuration space by the gradient operator $(\nabla_1 \cdot \nabla_2)$. Similarly, the two-pion loop contribution, as shown in the right diagram of Figure 2 reads

$$V_{2\pi-loop}(r_1, r_2) = \frac{1}{16f_\pi^4} \int \int \frac{d^3\mathbf{k}_1 d^3\mathbf{k}_2}{(2\pi)^6} e^{i\mathbf{k}_1\mathbf{r}_1}e^{i\mathbf{k}_2\mathbf{r}_2}f(\mathbf{k}_1^2)f(\mathbf{k}_2^2)A. \quad (46)$$

Here, $A = -\frac{1}{2E_{\mathbf{k}_1}} - \frac{1}{2E_{\mathbf{k}_2}} + \frac{2}{E_{\mathbf{k}_1} + E_{\mathbf{k}_2}}$. Expressing Eqs. (45) and (46) in the integral representation of $E_{\mathbf{k}_1}$, and making the Fourier transformation, one can then obtain the corresponding potentials.

3 Numerical Analysis

With the central potentials obtained in preceding section, one can calculate the heavy baryonium spectrum by solving the Schrödinger equation. In our numerical evaluation, the Matlab based package Matslise [31] is employed. The following inputs from Particle

Data Book [32] are used in the numerical calculation:

$$M_{\Lambda_c^+} = 2.286\text{GeV} , \ M_{\Sigma_c^0} = 2.454\text{GeV} , \ M_{\Sigma_c^*} = 2.518\text{GeV} , \ f_\pi = 0.132\text{GeV} , \ m = 0.135\text{GeV} , \quad (47)$$

and both spin- $\frac{1}{2}$ and $-\frac{3}{2}$ fermion intermediates are taken into account.

It is obvious that the main uncertainties in the evaluation of heavy baryonium remain in the couplings of Eq. (17). The magnitudes of the two independent couplings g_1 and g_2 were phenomenologically analyzed in Ref. [25], and two choices for them were suggested, i.e.,

$$g_1 = \frac{1}{3} , \ g_2 = -\sqrt{\frac{2}{3}} \quad (48)$$

and

$$g_1 = \frac{1}{3} \times 0.75 , \ g_2 = -\sqrt{\frac{2}{3}} \times 0.75 , \quad (49)$$

which implies the g_4 lies in the scope of 1 to 1.4, similar as estimated by Ref. [30] in the chiral limit.

3.1 Gaussian form factor case

The central potential from two-pion exchange box which can be regularized by widely used Gaussian form factor $f(\mathbf{k}^2) = e^{-\mathbf{k}^2/\Lambda^2}$ reads

$$\begin{aligned} V_{CG}^B(r_1, r_2) &= - \left(\frac{g_4^4}{f_\pi^4} \right) \left[\frac{1}{\pi} \int_0^\infty \frac{d\lambda}{\Delta_1^2 + \lambda^2} O_1(\mathbf{k}_1, \mathbf{k}_2) F(\lambda, r_1) F(\lambda, r_2) \right. \\ &\quad \left. - \frac{2\Delta_1}{\pi^2} O_1(\mathbf{k}_1, \mathbf{k}_2) \int_0^\infty \frac{d\lambda}{\Delta_1^2 + \lambda^2} F(\lambda, r_1) \int_0^\infty \frac{d\lambda}{\Delta_1^2 + \lambda^2} F(\lambda, r_2) \right] \\ &= \sum_i V_{CGi}^B + \dots . \end{aligned} \quad (50)$$

Details of the derivation of Eq. (50) from Eq. (42) can be found in the Appendix. There, the function $F(\lambda, r)$ is defined by Eq. (72). And, similarly the central potential from two-pion exchange crossed diagram gives

$$\begin{aligned} V_{CG}^C(r_1, r_2) &= - \left(\frac{g_4^4}{f_\pi^4} \right) \left[\frac{1}{\pi} \int_0^\infty \frac{d\lambda (\Delta_1^2 - \lambda^2)}{(\Delta_1^2 + \lambda^2)^2} O_1(\mathbf{k}_1, \mathbf{k}_2) F(\lambda, r_1) F(\lambda, r_2) \right] \\ &= \sum_i V_{CGi}^C + \dots . \end{aligned} \quad (51)$$

Here, the ellipsis represents the high singular terms in $r_2 \rightarrow r_1 = r$ limit, which behave as higher order corrections to the potential and will not be taken into account in this work, but will be discussed elsewhere. The central potential of Eq. (50) is obtained in the case of spin- $\frac{3}{2}$ intermediate state, and the explicit forms of V_{CGi} from box diagram are

$$V_{CG1}^B = -\frac{g_4^4 \Lambda^7}{128\sqrt{2}\pi^{7/2}f_\pi^4\Delta_1^2}e^{-\frac{\Lambda^2 r^2}{2}}, \quad (52)$$

$$V_{CG2}^B = -\frac{g_4^4 \Lambda^5}{16\sqrt{2}\pi^{7/2}f_\pi^4\Delta_1^2 r^2}e^{-\frac{\Lambda^2 r^2}{2}}, \quad (53)$$

$$V_{CG3}^B = \frac{g_4^4 \Lambda^3 m^{5/2} e^{m^2/\Lambda^2}}{32\sqrt{2}\pi^3 f_\pi^4 \Delta_1^2 r^{3/2}}e^{-\frac{\Lambda^2 r^2}{4}-mr}, \quad (54)$$

$$V_{CG4}^B = \frac{g_4^4 \Lambda^3 m^{3/2} e^{m^2/\Lambda^2}}{16\sqrt{2}\pi^3 f_\pi^4 \Delta_1^2 r^{5/2}}e^{-\frac{\Lambda^2 r^2}{4}-mr} - \frac{g_4^4 m^{9/2} e^{2m^2/\Lambda^2}}{128\pi^{5/2} f_\pi^4 \Delta_1^2 r^{5/2}}e^{-2mr}. \quad (55)$$

With Gaussian form factors it is seen from Eq. (72) in the Appendix that for a given Λ the function $F(\lambda, r)$ is suppressed for large λ values, that is the dominant contribution to potential comes from the small λ region. So, in obtaining the analytic expressions of above potentials and hereafter, we expand the corresponding functions, as defined in the Appendix, in λ and keep only the leading term. In this approach, the crossed diagram contributes to the potential the same as the box diagram at the leading order in λ expansion, and hence is not presented here.

Similarly, we obtain the potentials from triangle and two-pion loop diagrams, i.e.,

$$\begin{aligned} V_{CG5}^T &= \frac{g_4^2 m \Lambda^3}{32\sqrt{2}\pi^{7/2}f_\pi^4\Delta_1 r^2}e^{-\frac{\Lambda^2 r^2}{2}} - \frac{g_4^2 m^{5/2} \Lambda e^{m^2/\Lambda^2}}{16\sqrt{2}\pi^3 f_\pi^4 \Delta_1 r^{5/2}}e^{-\frac{\Lambda^2 r^2}{4}-mr} \\ &+ \frac{g_4^2 m^{7/2} e^{2m^2/\Lambda^2}}{128\pi^{5/2} f_\pi^4 \Delta_1 r^{5/2}}e^{-2mr}, \end{aligned} \quad (56)$$

and

$$V_{CG6}^L = -\frac{m^{1/2} \Lambda^3}{32\sqrt{2}\pi^2 f_\pi^4 r^{3/2}}e^{-\frac{1}{4}\Lambda^2 r^2 - mr}. \quad (57)$$

To get the central potential for the case of spin- $\frac{1}{2}$ intermediate state, one needs only to make the following replacement

$$g_4 \rightarrow g_2, \quad \Delta_1 \rightarrow \Delta'_1 = M_{\Sigma_c} - M_{\Lambda_c} \quad (58)$$

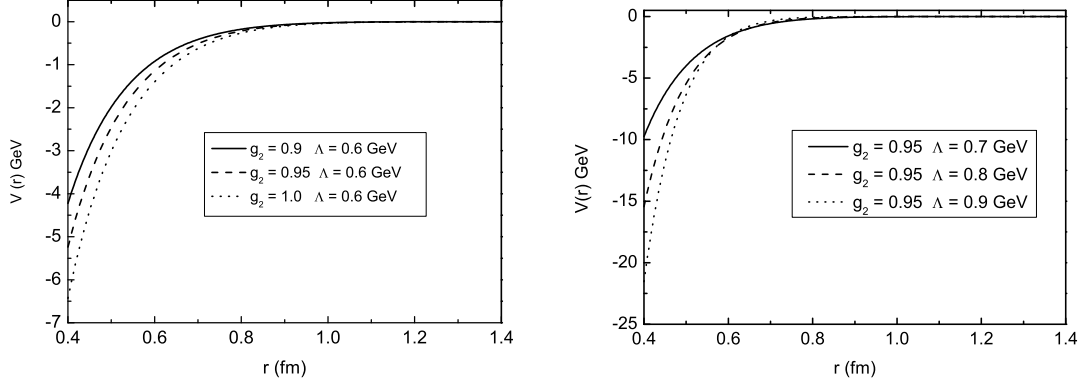


Figure 3: The Λ_c - $\bar{\Lambda}_c$ central potential behavior in case of Gaussian form factor versus different parameter choices.

in Eq.(50).

Note that in above asymptotic expressions we keep only those terms up to order $\frac{1}{r^{5/2}}$, and more singular terms are not taken into account in this work. The dependence of potential with various parameters are shown in Figure 3. The results indicate that the potential approaches to zero quickly in long range in every case, while in short range the potential diverges very much with different parameters, as expected. As a result, the binding energy heavily depends on input parameters, the coupling constants and cutoff. One can read from the figure that in the small coupling situation, the potential becomes too narrow and shallow to bind two heavy baryons. Table 2 presents the binding energies of Λ_c - $\bar{\Lambda}_c$ and Σ_c - $\bar{\Sigma}_c$ systems with different inputs. Schematically, the radial wave functions for the ground state of Λ_c - $\bar{\Lambda}_c$ system with Gaussian and monopole form factors are shown in Figure 4 respectively, while the wave functions for Σ_c - $\bar{\Sigma}_c$ system exhibit similar curves.

3.2 Monopole form factor case

In order to regulate the singularities at the origin in configuration space, usually people employ three types form factors in the literature, i.e. the Gaussian, the monopole, and the

Table 2: Binding energies with different inputs with Gaussian form factor. The left table is for the $\Lambda_c\text{-}\bar{\Lambda}_c$ system, and the right one for $\Sigma_c\text{-}\bar{\Sigma}_c$ system.

$ g_2 $	$\Lambda(\text{GeV})$	Binding energy	Baryonium mass	g_1	$\Lambda(\text{GeV})$	Binding energy	Baryonium mass
<0.9	<0.6	No	-	<1.0	<0.8	No	-
0.9	0.6	-22 MeV	4.550 GeV	1.0	0.8	-11 MeV	4.895 GeV
0.95	0.6	-77 MeV	4.495 GeV	1.05	0.8	-61 MeV	4.845 GeV
1.0	0.6	-168 MeV	4.404 GeV	1.1	0.8	-145 MeV	4.761 GeV
0.95	0.7	-196 MeV	4.376 GeV	1.05	0.85	-141 MeV	4.765 GeV
0.95	0.8	-227 MeV	4.345 GeV	1.05	0.9	-266 MeV	4.640 GeV
0.95	0.9	-588 MeV	3.984 GeV	1.05	0.95	-438 MeV	4.468 GeV

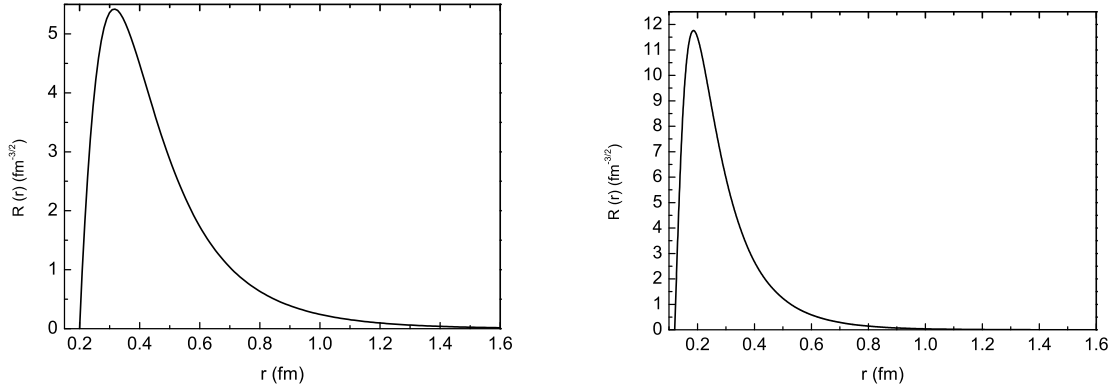


Figure 4: Radial wave function of $\Lambda_c\text{-}\bar{\Lambda}_c$ ground state. The left figure is for case of Gaussian form factor under the condition of $|g_2| = 0.95$ and $\Lambda = 0.8$, and the right one is for the case of monopole form factor with $|g_2| = 0.9$ and $\Lambda = 0.95$.

dipole form factors [34]. For comparison we also calculate the potential with monopole form factor using the same factorization technique, and the basic Fourier transformation for monopole form factor is presented in Appendix for the sake of convenience. Here, in obtaining the analytic expressions for potentials we also take the measure of expanding the corresponding functions in parameter λ and keeping only the leading term. Then, what obtained from the box-diagram contribution reads

$$\begin{aligned}
V_{CM}^B(r) = & - \frac{g_4^4}{8\pi^{5/2}f_\pi^4\Delta^2r^{5/2}} \left(\frac{m^{9/2}}{4}e^{-2mr} + \frac{\Lambda^4m^{1/2}}{4}e^{-2\Lambda r} \right) \\
& + \frac{g_4^4\Lambda^{5/2}m^{5/2}}{8\sqrt{2}\pi^{5/2}f_\pi^4\sqrt{m+\Lambda}\Delta_1^2r^{5/2}} e^{-(m+\Lambda)r} .
\end{aligned} \tag{59}$$

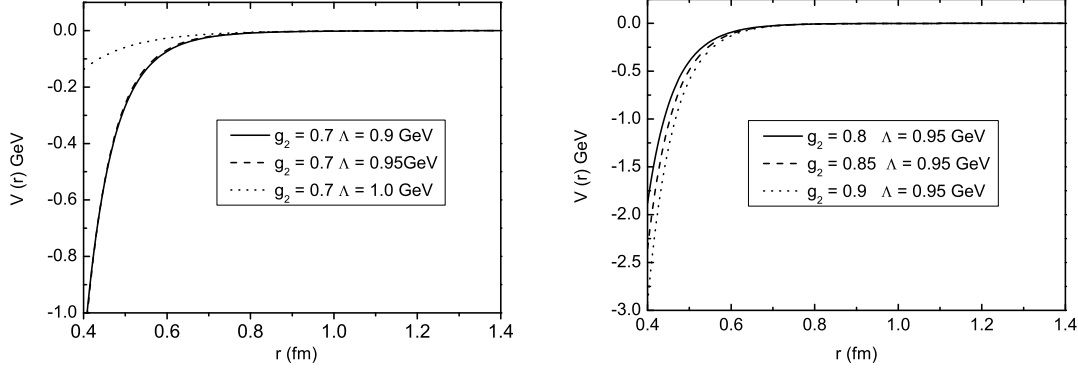


Figure 5: The $\Lambda_c\text{-}\bar{\Lambda}_c$ central potential behavior in case of monopole form factor versus different choices of inputs.

Contributions from triangle and two-pion loop diagrams are

$$\begin{aligned}
 V_{CM}^T(r) = & \frac{g_4^2 m^{7/2}}{16\pi^{5/2} f_\pi^4 \Delta_1 r^{5/2}} e^{-2mr} + \frac{g_4^2 m \Lambda^{5/2}}{16\pi^{5/2} f_\pi^4 \Delta_1 r^{5/2}} e^{-2\Lambda r} \\
 & - \frac{g_4^2 m^{5/2} \Lambda^{3/2}}{4\sqrt{2}\pi^{5/2} f_\pi^4 \sqrt{m + \Lambda} \Delta_1 r^{5/2}} e^{-(m+\Lambda)r}
 \end{aligned} \tag{60}$$

and

$$V_{CM}^L(r) = -\frac{(\Lambda^2 - m^2) m^{1/2}}{32\sqrt{2}\pi^{3/2} f_\pi^4 r^{3/2}} e^{-(m+\Lambda)r} + \frac{(\Lambda^2 - m^2) \Lambda^{1/2}}{32\sqrt{2}\pi^{3/2} f_\pi^4 r^{3/2}} e^{-2\Lambda r} \tag{61}$$

respectively, where superscript B , T , and L stand for box, triangle and 2π loop. Note that since there is no heavy baryon intermediate state in the 2π loop process, as shown in the right graph of Figure 2, the potential range of it appears different.

We find that the structure of potential with monopole form factor is much simpler than the Gaussian case. The dependence of potential with various parameters are shown in Fig.5. From the figure one can see that in small coupling case the potential change less, which means the potential tends to be insensitive to the small coupling, and hence the binding energy. Solving the Schrödinger equation we then obtain eigenvalues for different input parameters, given in Table 3. From the table, we notice that the binding energy is sensitive to and changes greatly with the variation of g_1 , $|g_2|$ and the cutoff Λ , the same as the case with Gaussian form factor. Intuitively, the realistic baryonium can only accommodate small ones of those parameters.

Table 3: Binding energies with different inputs with monopole form factor. The left table is for the $\Lambda_c\text{-}\bar{\Lambda}_c$ system, and the right one for $\Sigma_c\text{-}\bar{\Sigma}_c$ system.

$ g_2 $	$\Lambda(\text{GeV})$	Binding energy	Baryonium mass	g_1	$\Lambda(\text{GeV})$	Binding energy	Baryonium mass
<0.7	<0.9	No	-	< 0.9	< 0.9	No	-
0.8	0.95	-117 MeV	4.455 GeV	0.95	0.95	-438 MeV	4.468 GeV
0.85	0.95	-420 MeV	4.152 GeV	1.0	0.95	-830 MeV	4.076 GeV
0.9	0.95	-521 MeV	4.051 GeV	1.05	0.95	-1003 MeV	3.903 GeV
0.7	0.9	-5 MeV	4.567 GeV	0.9	0.9	-40 MeV	4.866 GeV
0.7	0.95	-67 MeV	4.505 GeV	0.9	0.95	-153 MeV	4.753 GeV
0.7	1.0	-252 MeV	4.320 GeV	0.9	1.0	-345 MeV	4.561 GeV

3.3 Ground state of $\Lambda_b\text{-}\bar{\Lambda}_b$ baryonium

Table 4: Binding energies with the change of parameters for $\Lambda_b\text{-}\bar{\Lambda}_b$ system. The left table is for the Gaussian form factor, and the right one for the monopole form factor. Here g_b corresponds to g_2 in charmed baryonium sector

$ g_b $	$\Lambda(\text{GeV})$	binding energy	Baryonium mass	$ g_b $	$\Lambda(\text{MeV})$	Binding energy	Baryonium mass
<0.7	<0.7	No	No	< 1.0	< 0.8	No	No
0.7	0.75	-4 MeV	11.236 GeV	1.0	0.8	-11 MeV	11.229 GeV
0.8	0.75	-76 MeV	11.164 GeV	1.05	0.8	-56 MeV	11.184 GeV
0.9	0.75	-294 MeV	10.946 GeV	1.1	0.8	-143 MeV	11.097 GeV
0.8	0.8	-164 MeV	11.706 GeV	1.05	0.8	-103 MeV	11.137 GeV
0.8	0.9	-396 MeV	10.844 GeV	1.05	0.9	-164 MeV	11.076 GeV
0.8	1.0	-622 MeV	10.618 GeV	1.05	1.0	-321 MeV	10.919 GeV

We also estimate the ground state of $\Lambda_b\text{-}\bar{\Lambda}_b$ baryonium system with Gaussian and monopole form factors. The result are shown in Table 4, where g_b corresponds to g_2 in charmed baryonium sector. Note that since the dominant decay mode of Σ_b is to $\Lambda_b\pi$, by which we may constrain the $\Sigma_b\Lambda_b\pi$ coupling from the experiment result, and this may shed lights on the further investigation on the nature of possible baryonium.

4 Summary and Conclusions

In the framework of heavy baryon chiral perturbation theory we have studied the heavy baryon-baryon interaction, and obtained the interaction potential, the central potential, in the case of two-pion exchange. The Gaussian and monopole types form factors are employed to regularized the loop integrals in the calculation. As a leading order analysis, the tensor potential and higher order contributions in $\frac{1}{M_H}$ expansion are neglected. As expected, we found that the potential is sensitive to the baryon-pion couplings and the energy cutoff Λ used in the form factor.

We apply the obtained potential to the Schrödinger equation in attempting to see whether the attraction of two-pion-exchange potential is large enough to constrain two heavy baryons into a baryonium. We find it true for a reasonable choice of cutoff Λ and baryon-pion couplings, which is quite different from the conclusion of a recent work in the study of $D\bar{D}$ potential through two-pion exchange [35]. Since usually the cutoff Λ is taken to be less than the nucleon mass, i.e. about 1 GeV in the literature, in our calculation we adopt a similar value employed in the nucleon-nucleon case. In Ref. [35] authors took a fixed coupling $g = 0.59$ and obtained the binding with a large cutoff. While in our calculation for the baryonium system with Gaussian form factor, there will be no binding in case $g_1 < 1.0$ and $\Lambda < 0.8$. The increase of coupling constant will lead to an even smaller Λ for a given binding energy.

Based on our calculation results it is interesting to note that in case there exists binding in $\Sigma_c\text{-}\bar{\Sigma}_c$ system, with both Gaussian and monopole factors, the coupling g_1 will be much bigger than what conjectured in Ref. [25]. However, for $\Lambda_c\text{-}\bar{\Lambda}_c$ system, to form a bound state the baryon-Goldstone coupling g_2 could be similar in magnitude as what estimated in the literature.

Notice that the potential depends not only on coupling constants and cutoff Λ , it also depends on the types of form factors employed. Our calculation indicates that the Gaussian form factor and Monopole form factor are similar in regulating the singularities at origin, and lead to similar results, with only subtle difference, for both Λ_c and Λ_b systems. Numerical result tells that the heavy baryon-baryon potentials are more sensitive

to the coupling constants in the case of Monopole form factor, but more sensitive to the cutoff Λ in the case of Gaussian form factor. From our calculation it is tempting to conjecture that the recently observed states $Y(4260)$ and $Y(4360)$, but not $Y(4660)$ [6], in charm sector could be a $\Lambda_c\bar{\Lambda}_c$ bound state with reasonable amount of binding energy, which deserves a further investigation. Our result also tells that the newly observed “exotic” state in bottom sector, the $Y_b(10890)$ [37], could be treated as the $\Lambda_b\bar{\Lambda}_b$ bound state, whereas with an extremely large binding energy.

It is worth emphasizing at this point that although our calculation result favors the existence of heavy baryonium, it is still hard to make a definite conclusion yet, especially with only the leading order two-pion-exchange potential. The potential sensitivity on coupling constants and energy cutoff also looks unusual and asks for further investigation. To be more closer to the truth, one needs to go beyond the leading order of accuracy in $\frac{1}{M_H}$ expansion; one should also investigate the potential while two baryon-like triquark clusters carry colors as proposed in the heavy baryonium model [11, 16]; last, but not least, the unknown and difficult to evaluate annihilation channel effect on the heavy baryonium potential should also be clarified, especially for heavy baryon-antibaryon interaction, which nevertheless could be phenomenologically parameterized so to reproduce known widths of some observed states.

Acknowledgments

This work was supported in part by the National Natural Science Foundation of China (NSFC) and by the CAS Key Projects KJCX2-yw-N29 and H92A0200S2.

Appendix

In this Appendix, we present more detailed formulas and definitions used for the sake of reader's convenience.

The γ matrices take the following convention

$$\gamma^0 = \begin{pmatrix} 1 & 0 \\ 0 & -1 \end{pmatrix}, \quad \gamma^i = \begin{pmatrix} 0 & \sigma^i \\ -\sigma^i & 0 \end{pmatrix}, \quad \gamma_5 = \begin{pmatrix} 0 & 1 \\ 1 & 0 \end{pmatrix}. \quad (62)$$

And the Dirac spinors for Σ_c read as

$$u(p) = \sqrt{\frac{E + M_\Sigma}{2M_\Sigma}} \begin{pmatrix} \chi_a \\ \frac{\boldsymbol{\sigma} \cdot \mathbf{p}}{E + M_\Sigma} \chi_a \end{pmatrix}, \quad (63)$$

where χ_a is two-component Pauli spinor, and

$$v(p) = \sqrt{\frac{E + M_\Sigma}{2M_\Sigma}} \begin{pmatrix} \frac{\boldsymbol{\sigma} \cdot \mathbf{p}}{E + M_\Sigma} \eta_a \\ \eta_a \end{pmatrix}, \quad (64)$$

where $\eta_a = -i\sigma^2 \chi_a^*$, and $a = 1, 2$. Spin- $\frac{3}{2}$ field for Σ^{+*} is described by Rarita-Schwinger spinor $u^\mu(p, \sigma)$, which can be constructed by spin-1 vector and spin- $\frac{1}{2}$ field [36], that is

$$u^\mu = \sqrt{\frac{E + M_{\Sigma^{+*}}}{2M_{\Sigma^{+*}}}} L^{(1)}(p)_\nu^\mu \begin{pmatrix} 1 \\ \frac{\boldsymbol{\sigma} \cdot \mathbf{p}}{E + M_{\Sigma^{+*}}} \end{pmatrix} S^{\dagger\nu} \psi(\sigma), \quad (65)$$

where $\psi(\sigma)$ is four-component Pauli spinor of a spin- $\frac{3}{2}$ particle, and $L^{(1)}(p)_\nu^\mu$ is the boost operator for spin-1 particle,

$$L^{(1)}(p)_\nu^\mu = \begin{pmatrix} \frac{E}{M_{\Sigma^{+*}}} & \frac{p_j}{M_{\Sigma^{+*}}} \\ \frac{p_i}{M_{\Sigma^{+*}}} & \delta_j^i - \frac{p^i p_j}{M_{\Sigma^{+*}}(E + M_{\Sigma^{+*}})} \end{pmatrix}, \quad (66)$$

where i, j are indices of the space components of momentum p . The positive- and negative-energy projection operators for spin- $\frac{1}{2}$ baryon are

$$[\Lambda^+(p)]_{\alpha\beta} = \sum_{\pm s} u_\alpha(p, s) \bar{u}_\beta(p, s) = \left(\frac{\not{p} + M_{\Sigma_c}}{2M_{\Sigma_c}} \right)_{\alpha\beta} \quad (67)$$

and

$$[\Lambda^-(p)]_{\alpha\beta} = - \sum_{\pm s} v_\alpha(p, s) \bar{v}_\beta(p, s) = \left(\frac{-\not{p} + M_{\Sigma_c}}{2M_{\Sigma_c}} \right)_{\alpha\beta}, \quad (68)$$

respectively.

The positive- and negative-energy projection operators for spin- $\frac{3}{2}$ baryon are

$$\begin{aligned} [\Lambda_{\mu\nu}^+(p)]_{\alpha\beta} &= \sum_{\pm s} u_{\mu, \alpha}(p, s) \bar{u}_{\nu, \beta}(p, s) \\ &= [\frac{\not{p} + M_{\Sigma_c^*}}{2M_{\Sigma_c^*}}]_{\alpha\beta} \left(g_{\mu\nu} - \frac{\gamma_\mu \gamma_\nu}{3} - \frac{2p_\mu p_\nu}{3M_{\Sigma_c^*}^2} + \frac{p_\mu \gamma_\nu - p_\nu \gamma_\mu}{3M_{\Sigma_c^*}} \right), \end{aligned} \quad (69)$$

and

$$\begin{aligned} [\Lambda_{\mu\nu}^-(p)]_{\alpha\beta} &= - \sum_{\pm s} v_{\mu, \alpha}(p, s) \bar{v}_{\nu, \beta}(p, s) \\ &= [\frac{-\not{p} + M_{\Sigma_c^*}}{2M_{\Sigma_c^*}}]_{\alpha\beta} \left(g_{\mu\nu} - \frac{\gamma_\mu \gamma_\nu}{3} - \frac{2p_\mu p_\nu}{3M_{\Sigma_c^*}^2} + \frac{p_\mu \gamma_\nu - p_\nu \gamma_\mu}{3M_{\Sigma_c^*}} \right), \end{aligned} \quad (70)$$

respectively. Here, μ and ν are Lorentz indices; α and β are Dirac spinor indices.

The basic Fourier transformation with Gaussian form factor reads

$$\begin{aligned} I_2(m, r) &= \int_{-\infty}^{\infty} \frac{d^3\mathbf{k}}{(2\pi)^3} \frac{e^{i\mathbf{k}\mathbf{r}} e^{-\mathbf{k}^2/\Lambda^2}}{\mathbf{k}^2 + m^2} \\ &= \frac{1}{8\pi r} e^{m^2/\Lambda^2} \left[e^{-mr} \operatorname{erfc} \left(-\frac{\Lambda r}{2} + \frac{m}{\Lambda} \right) - e^{mr} \operatorname{erfc} \left(\frac{\Lambda r}{2} + \frac{m}{\Lambda} \right) \right], \end{aligned} \quad (71)$$

and hence

$$F(\lambda, r) = \int \frac{d^3\mathbf{k}}{(2\pi)^3} \frac{e^{i\mathbf{k}\mathbf{r}} e^{-\mathbf{k}^2/\Lambda^2}}{\mathbf{k}^2 + m^2 + \lambda^2} = I_2(\sqrt{m^2 + \lambda^2}, r) e^{-\lambda^2/\Lambda^2}. \quad (72)$$

$\operatorname{erfc}(x)$ is complementary error function, which is defined as

$$\operatorname{erfc}(x) = \frac{2}{\sqrt{\pi}} \int_x^{\infty} e^{-t^2} dt. \quad (73)$$

The factorization in double Fourier transformation goes like

$$\begin{aligned} H_{11} &= \int \int \frac{d^3\mathbf{k}_1 d^3\mathbf{k}_2}{(2\pi)^6} \frac{e^{i\mathbf{k}_1\mathbf{r}_1} e^{i\mathbf{k}_2\mathbf{r}_2} f(\mathbf{k}_1^2) f(\mathbf{k}_2^2)}{\omega_1 \omega_2 (\omega_1 + a) (\omega_2 + a) (\omega_1 + \omega_2)} \\ &= \int \int \frac{d^3\mathbf{k}_1 d^3\mathbf{k}_2}{(2\pi)^6} \frac{1}{a^2} \left[\frac{2}{\pi} \int_0^{\infty} \frac{e^{i\mathbf{k}_1\mathbf{r}_1} e^{i\mathbf{k}_2\mathbf{r}_2} f(\mathbf{k}_1^2) f(\mathbf{k}_2^2) d\lambda}{(\omega_1^2 + \lambda^2) (\omega_2^2 + \lambda^2)} \right. \\ &\quad \left. - \frac{2}{\pi} \int_0^{\infty} \frac{e^{i\mathbf{k}_1\mathbf{r}_1} e^{i\mathbf{k}_2\mathbf{r}_2} f(\mathbf{k}_1^2) f(\mathbf{k}_2^2) \lambda^2 d\lambda}{(a^2 + \lambda^2) (\omega_1^2 + \lambda^2) (\omega_2^2 + \lambda^2)} \right] - \frac{1}{a} G_{11}(\lambda, r_1) G_{11}(\lambda, r_2) \\ &= \frac{2}{\pi} \int_0^{\infty} \frac{d\lambda}{a^2 + \lambda^2} F(\lambda, r_1) F(\lambda, r_2) - \frac{1}{a} G_{11}(\lambda, r_1) G_{11}(\lambda, r_2). \end{aligned} \quad (74)$$

$$= \frac{2}{\pi} \int_0^{\infty} \frac{d\lambda}{a^2 + \lambda^2} F(\lambda, r_1) F(\lambda, r_2) - \frac{1}{a} G_{11}(\lambda, r_1) G_{11}(\lambda, r_2). \quad (75)$$

Here,

$$\begin{aligned}
G_{11} &= \int \frac{d^3 \mathbf{k}_1}{(2\pi)^3} \frac{e^{i\mathbf{k}_1 \mathbf{r}} e^{-\mathbf{k}_1^2/\Lambda^2}}{\omega_1(\omega_1 + a)} = \int \frac{d^3 \mathbf{k}_1}{(2\pi)^3} \frac{2a}{\pi} \int_0^\infty \frac{e^{i\mathbf{k}_1 \mathbf{r}} e^{-\mathbf{k}_1^2/\Lambda^2} d\lambda}{(a^2 + \lambda^2)(\omega_1^2 + \lambda^2)} \\
&= \frac{2a}{\pi} \int_0^\infty \frac{d\lambda}{(a^2 + \lambda^2)} F(\lambda, r), \tag{76}
\end{aligned}$$

and for simplicity we define $\omega_1 = \sqrt{\mathbf{k}_1^2 + m^2}$ and $\omega_2 = \sqrt{\mathbf{k}_2^2 + m^2}$.

In the case of the monopole form factor, i.e. $f(\mathbf{k}^2) = \frac{\Lambda^2 - m^2}{\Lambda^2 + \mathbf{k}^2}$, the corresponding function to $F(\lambda, r)$ reads

$$\begin{aligned}
R(\lambda, r) &= \int \frac{d^3 \mathbf{k}}{(2\pi)^3} \frac{e^{i\mathbf{k} \mathbf{r}}}{\mathbf{k}^2 + m^2 + \lambda^2} \frac{\Lambda^2 - m^2}{\Lambda^2 + \mathbf{k}^2 + \lambda^2} \\
&= \frac{1}{4\pi r} \left(e^{-r\sqrt{m^2 + \lambda^2}} - e^{-r\sqrt{\Lambda^2 + \lambda^2}} \right). \tag{77}
\end{aligned}$$

Operator $O_1(\mathbf{k}_1, \mathbf{k}_2)$ contains two parts. The first part of $O_1(\mathbf{k}_1, \mathbf{k}_2)$ while acting on functions in configuration space goes like

$$\begin{aligned}
O_1(\mathbf{k}_1, \mathbf{k}_2) F(\lambda, r_1) F(\lambda, r_2) &= (\mathbf{k}_1 \cdot \mathbf{k}_2)^2 F(\lambda, r_1) F(\lambda, r_2) \\
&= (\nabla_{1i} \nabla_{1j}) F(\lambda, r_1) (\nabla_{2i} \nabla_{2j}) F(\lambda, r_2) \\
&= \frac{2}{r^2} F'(\lambda, r) F'(\lambda, r) + F''(\lambda, r) F''(\lambda, r), \tag{78}
\end{aligned}$$

where

$$\nabla_i \nabla_j = \left(\delta_{ij} - \frac{x_i x_j}{r^2} \right) \left(\frac{1}{r} \frac{d}{dr} \right) + \frac{x_i x_j}{r^2} \left(\frac{d^2}{dr^2} \right), \tag{79}$$

and the limit $r_2 \rightarrow r_1 = r$ is taken. The second part of $O_2(\mathbf{k}_1, \mathbf{k}_2)$ while acting on functions in configuration space goes like

$$\begin{aligned}
O_2(\mathbf{k}_1, \mathbf{k}_2) F(\lambda, r_1) F(\lambda, r_2) &= (\boldsymbol{\sigma}_1 \cdot \mathbf{k}_1 \times \mathbf{k}_2) (\boldsymbol{\sigma}_2 \cdot \mathbf{k}_1 \times \mathbf{k}_2) F(\lambda, r_1) F(\lambda, r_2) \\
&= \sigma_{1i} \sigma_{2j} \varepsilon_{ikl} \varepsilon_{jmn} (\nabla_{1k} \nabla_{1m}) F(\lambda, r_1) (\nabla_{2l} \nabla_{2n}) F(\lambda, r_2) \\
&= \sigma_{1i} \sigma_{2j} (\delta_{ij} \delta_{km} \delta_{ln} + \delta_{im} \delta_{kn} \delta_{lj} + \delta_{in} \delta_{lm} \delta_{kj} \\
&\quad - \delta_{lj} \delta_{km} \delta_{in} - \delta_{lm} \delta_{kn} \delta_{ij} - \delta_{ln} \delta_{im} \delta_{kj}) \times \\
&\quad (\nabla_{1k} \nabla_{1m}) F(\lambda, r_1) (\nabla_{2l} \nabla_{2n}) F(\lambda, r_2) \\
&= \frac{2}{3} \left[\frac{1}{r^2} F'(\lambda, r) F'(\lambda, r) + \frac{2}{r} F'(\lambda, r) F''(\lambda, r) \right] (\boldsymbol{\sigma}_1 \cdot \boldsymbol{\sigma}_2) \\
&\quad + \frac{2}{3} \left(\frac{F'(\lambda, r)}{r} - F''(\lambda, r) \right) \frac{1}{r} F'(\lambda, r) S_{12}, \tag{80}
\end{aligned}$$

where $\boldsymbol{\sigma}_1 \cdot \boldsymbol{\sigma}_2$ gives spin-spin potential and $S_{12} = \frac{3(\boldsymbol{\sigma}_1 \cdot \mathbf{r})(\boldsymbol{\sigma}_2 \cdot \mathbf{r})}{r^2} - \boldsymbol{\sigma}_1 \cdot \boldsymbol{\sigma}_2$ gives the tensor potential.

References

- [1] Wolfgang Lucha, Franz F. Schöberl, and Dieter Gromes, Phys. Rept. **200**, 127 (1991).
- [2] C. Quigg and Jonathan L. Rosner, Phys. Rept. **56**, 167 (1979).
- [3] V.A. Novikov, L.B. Okun, M.A. Shifman, A.I. Vainshtein, M.B. Voloshin and V.I. Zakharov, Phys. Rept. **41**, 1 (1978).
- [4] S.K.Choi *et al.* (Belle Collaboration), Phys. Rev. Lett. **91**,262001 (2003).
- [5] B. Aubert *et al.* (BarBar Collaboration), Phys, Rev D **77**,111101 (2008).
- [6] B. Aubert *et al.* (BarBar Collaboration), Phys, Rev Lett **98**, 212001 (2007); X. L. Wang *et al* Belle Collaboration), Phys. Rev. Lett. **99**, 142002 (2007); S. K. Choi *et al.* (Belle Collaboration), Phys. Rev. Lett. **100**, 142001 (2008); R. Mizuk *et al.* (Belle Collaboration), Phys. Rev. D**80**, 031104 (2009).
- [7] S. L. Zhu, Phys. Lett. B **625**, 212 (2005); E. Kou and O. Pene, Phys. Lett. B **631**, 164 (2005); F. E. Close and P. R. Page, Phys. Lett. B **628**, 215 (2005); X. Q. Luo and Y. Liu, Phys. Rev. D **74**, 034502 (2006); S. L. Zhu, Nucl. Phys. A **805**, 221c (2008); S. L. Zhu, Int. J. Mod. Phys. E **17**, 283 (2008).
- [8] X. Liu, X.Q. Zeng, and X.Q. Li, Phys. Rev. D **72**, 054023 (2005).
- [9] F.J. Llanes-Estrada, Phys. Rev. D **72**, 031503 (2005).
- [10] C.-Z. Yuan, P. Wang, and X.H. Mo, Phys. Lett. B **634**, 399 (2006).
- [11] C.-F. Qiao, Phys. Lett. B **639**, 263 (2006).
- [12] G.-J. Ding, Phys. Rev. D **79**, 014001 (2009).

- [13] L. Maiani, V. Riquer, F. Piccinini, and A. D. Polosa, Phys. Rev. D **72**, 031502(R) (2005).
- [14] G.-J. Ding, J.-J. Zhu, and M.-L. Yan, Phys. Rev. D **77**, 014033 (2008).
- [15] B.-Q. Li and K.-T. Chao, Phys. Rev. D **79**, 094004 (2009).
- [16] C.-F. Qiao, J. Phys. G: Nucl. Part. Phys. **35**, 075008 (2008).
- [17] D.V. Bugg, J. Phys. G: Nucl. Part. Phys. **36**, 075002 (2009).
- [18] F.-K. Guo, C. Hanhart, and U.-G. Meißner, Phys. Lett. B **665**, 26 (2008).
- [19] Z.-G. Wang and X.-H. Zhang, arXiv:0905.3784 [hep-ph].
- [20] A.M. Badalian, B.L.G. Bakker, and I.V. Danilkin, Phys. Atom. Nucl. **72**, 638 (2009).
- [21] R.M. Albuquerque and M. Nielsen, Nucl. Phys. A **815**, 53 (2009).
- [22] D. Ebert, R.N. Faustov, and V.O. Galkin, Eur. Phys. J. C **58**, 399 (2008).
- [23] N. Brambilla, *et al. Heavy quarkonium: progress, puzzles, and opportunities*, Eur. Phys. J. C **71**, 1534 (2011), arXiv:hep-ph/1010.5827.
- [24] N. Drenska, *et al. New Hadronic Spectroscopy*, Riv. Nuovo Cim. **033**, 633 (2010), arXiv:hep-ph/1006.2741.
- [25] Tung-Mow Yan, Y.C. Lin and Hoi-Lai Yu, Phys. Rev D**46**, 1148 (1992); Hai-Yang Cheng, Tung-Mow Yan *et al.* Phys. Rev D**47**, 1030 (1993).
- [26] A. Manohar and H. Georgi, Nucl. Phys. B **234**, 189 (1984).
- [27] Mark B. Wise, Phys. Rev. D **45**, R2188 (1992)
- [28] Th.A. Rijken and V.G.J. Stoks, Phys. Rev. C**46**, 73 (1992); Th.A. Rijken and V.G.J. Stoks, Phys. Rev. C**46**, 102 (1992);
- [29] Th.A. Rijken, Ann. Phys. **208**, 253 (1991).

- [30] D. Arndt, S.R. Beane and M.J. Savage, Nucl. Phys. A**726** 339, (2003); S.R. Beane and M.J. Savage, Phys. Lett. B **556**, 142 (2003).
- [31] <http://users.ugent.be/~vledoux/> .
- [32] K. Nakamura, *et al.*(Particle Data Group), J. Phys. G: Nucl. Part. Phys. **37**, 1 (2010).
- [33] Th.A. Rijken and V.G. Stoks, Phys. Rev. C**54**, 2869 (1996).
- [34] V.G.J. Stoks, R. A. M. Klomp, C. P. F. Terheggen and J. J. de Swart, Phys. Rev. C**49**, 2950 (1994).
- [35] Qing Xu, Gang Liu and Hong-Ying Jin, eprint, arXiv:hep-ph/1012.5949.
- [36] Th.A. Rijken and V.G. Stoks, Phys. Rev. C**46**, 102 (1992).
- [37] K.F. Chen, *et al.*, [Belle Collaboration], Phys. Rev. Lett. **100**, 112001 (2008).